Croatian Society for Materials Protection

Metalurgija/Metallurgy

Vol. 65 No. 3 / 2026

Improvement of Solidification Structure Uniformity in Al-Cu Alloy Casting Process

Xueting Li

https://doi.org/10.64486/m.65.3.10

School of Mechanical and Electronic Engineering, Yantai Institute of Science and Technology
Yantai 265600, China; lixueting2024@126.com

Type of the Paper: Article
Received: October 23, 2025
Accepted: January 9, 2026

Abstract: Aluminum–copper alloys are core lightweight materials in aerospace applications; however, their casting is prone to grain size imbalance and Al_2Cu phase segregation. To address these issues, this study focused on an Al–6.07 wt.% Cu alloy and employed a three-factor, three-level orthogonal experimental design using squeeze casting. The effects of pouring temperature, forming pressure, and holding time on solidification uniformity were investigated using metallographic microscopy, SEM, and EPMA. The results indicated that the optimal process parameters were a pouring temperature of 730 °C, a forming pressure of 170 MPa, and a holding time of 13 s, combined with aging at 120 °C for 4 h. Under these conditions, the grain size standard deviation (GSSD) of the surface and core was reduced to 7.3 μm and 13.5 μm, respectively, while the Al_2Cu phase segregation degree decreased to 0.14. Consequently, the tensile strength reached 342 MPa, with a microhardness of 120 HV. The study confirms that the proposed "pressure–temperature–solute" coupling mechanism effectively suppresses segregation, providing both theoretical insight and process guidance for the mass production of high-load-bearing alloy components.

Keywords: Al–Cu alloy; squeeze casting; solidification structure uniformity; process parameters; Al_2Cu phase

1. Introduction

Aluminum–copper (Al–Cu) alloys have become key materials for achieving structural lightweighting in high-end manufacturing sectors such as aerospace and new energy vehicles, owing to their high specific strength and excellent heat resistance. The uniformity of the solidification structure in cast components directly affects their safety and service life. However, achieving uniform solidification in high-performance Al–Cu alloy castings remains a major challenge. Grain size imbalance and second-phase segregation along grain boundaries lead to reduced mechanical stability, thereby limiting their application in high-load conditions [1–2]. Although conventional gravity casting can refine surface grains, it is ineffective in improving the core microstructure, resulting in limited overall uniformity enhancement [3]. Existing single external field control methods, such as extrusion or electromagnetic stirring, cannot completely suppress segregation and may introduce melt defects or provide insufficient mitigation of core grain coarsening [4]. Therefore, it is essential to address the lack of clear multi-parameter synergistic control mechanisms, the absence of quantitative evaluation methods for microstructural uniformity, and the incomplete understanding of the underlying microscopic

mechanisms, in order to establish a solid foundation for efficiently improving the solidification structure uniformity of Al–Cu alloys.

To investigate the formation mechanism of micropores during the solidification process of Al-Cu alloys, Yuan et al. simulated the formation of microstructures and micropores under different copper contents and solidification rates. The results showed that copper content affects the micropore morphology by changing the liquidus temperature, dendrite morphology, and hydrogen solubility, while the pull-out rate mainly changes the micropore characteristics by affecting hydrogen micropore nucleation [5]. When exploring the effect of casting technology on the uniformity of solidification structure of Al-Cu alloys, the Suprapto' team controlled the alloy properties by controlling the melting time. The study found that as the immersion time of copper in the aluminum liquid increased, the specific gravity and hardness of the cast hard aluminum increased significantly [6]. Meanwhile, a study by Peng and others on aluminum lithium alloys also provided a cross disciplinary reference case for the uniformity of solidification microstructure in Al-Cu alloys. This study found that preheating treatment can promote a finer and more uniform distribution of precipitated phases in alloys, effectively alleviating mechanical anisotropy. The subsequent aging treatment significantly improved the strength and toughness of the alloy by refining the grains and suppressing the formation of precipitation free zones [7].

In addition, Tan's research on aluminum silicon alloys also provided new ideas for exploring the influence of casting processes on the uniformity of solidification structure. To address the casting defects of the alloy, an improved cellular automaton model was developed by integrating thermodynamic and kinetic databases to simulate its solidification process. The model successfully predicted the morphology of α-Al dendrites in low-pressure casting and revealed the effect of cooling rate on the density of crystal nuclei and the uniformity of dendrite size. This study provided theoretical guidance for establishing the solidification microstructure performance relationship [8]. In summary, existing research has explored the solidification characteristics of aluminum-based alloys from the perspectives of component influence, single process regulation, and cross alloy reference, but has not solved the core issues of multi parameter synergy, quantitative characterization, and microscopic mechanisms. The 6.07 wt.% Cu content surpasses the solubility limit (5.6 wt.%) and typical commercial levels (3–5) wt.%, classifying it as a 'high-copper' alloy. This composition was selected to maximize precipitation strengthening while addressing the resultant solidification uniformity challenges. To address this challenge, a three factor three-level orthogonal experiment using squeeze casting was conducted, combined with multi-characterization techniques, to achieve precise control of process parameters on solidification uniformity.

The research aims to solve the bottleneck of solidification uniformity of high copper Al-Cu alloys, provide process support for their mass production in aerospace and new energy vehicle high load-bearing parts, and improve the theory of casting alloy uniformity control. The innovation of the research lies in using the holding time as the core variable, proposing a Grain Size Standard Deviation (GSSD) and a quantitative standard for Al_2Cu phase segregation, elucidating the coupling mechanism of "pressure field-temperature field-solute field", and providing theoretical and technical references for the stable improvement of alloy properties in the high-end manufacturing field.

2. Methods and Material

2.1. Characteristics of Al-Cu Alloy Matrix and Raw Material Specifications

High-copper Al-Cu alloys are widely used in aviation structural components due to their excellent mechanical properties [9], and their solidification structure uniformity is critical for component safety [10]. The study selected Al-6.07 wt.% Cu alloy as the object. The alloy composition was analyzed by Inductively Coupled Plasma Optical Emission Spectroscopy (ICP-OES). The measured Cu content was 6.02 wt.% – 6.11 wt.%, with impurity elements Fe ≤ 0.15 wt.% and Si ≤ 0.12 wt.%, and the balance was Al matrix. This composition design ensures sufficient Cu to form the Al_2Cu strengthening phase, while low impurity content prevents

https://doi.org/10.64486/m.65.3.10

brittle phase formation [11]. The detailed design composition and measured composition of the Al-Cu alloy are shown in Table 1.

Table 1. Design and measured composition of Al-Cu alloy

Sample No.	Al/wt.%	Cu/wt.%	Fe/wt.%	Si/wt.%	Others/wt.%
Designed Composition	Bal.	6.07	≤0.15	≤0.12	≤0.05
Measured Composition-1	Bal.	6.09	0.14	0.11	<0.05
Measured Composition-2	Bal.	6.02	0.13	0.09	<0.05
Measured Composition-3	Bal.	6.05	0.12	0.10	<0.05
Measured Composition-4	Bal.	6.11	0.15	0.12	<0.05
Measured Composition-5	Bal.	6.07	0.10	0.08	<0.05

The raw materials were selected from 99.97 % high-purity block-shaped pure Al ingots [12] and 99.95 % electrolytic copper wire [13]. The block shape of the Al ingots facilitates uniform heating, while the use of small-diameter copper wire ensures rapid dissolution and reduces compositional segregation.

2.2. Squeezing Casting Process Design and Sample Preparation

The melting process requires controlling the sequence of raw material addition, Ar gas flow rate, etc. to ensure the quality of the melt. The specific melting process is shown in Figure 1.

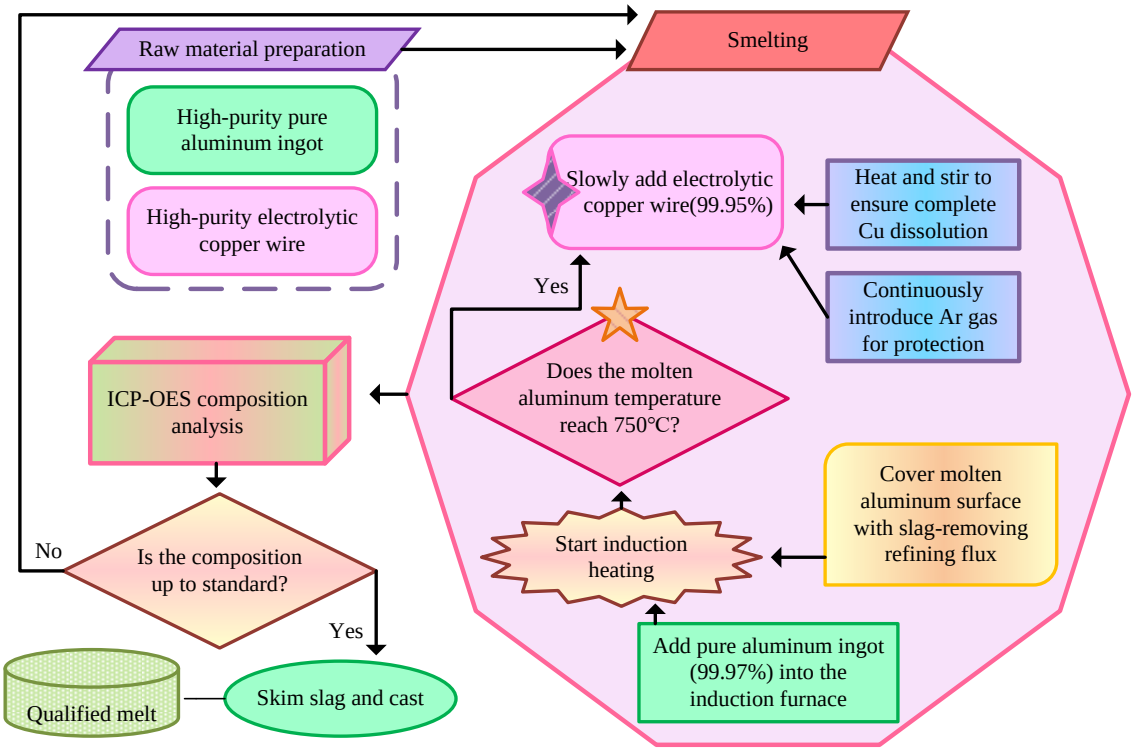

Figure 1. Schematic diagram of smelting process

https://doi.org/10.64486/m.65.3.10

As shown in Figure 1, the melting process ensures the production of high-quality melt with uniform composition and low gas content by controlling key parameters such as the order of raw material addition, temperature curve, and Ar gas protection flow rate [14]. The specific procedure involves first heating high-purity aluminum ingots in an induction furnace to 750 °C. Electrolytic copper wire is then slowly added and stirred until completely dissolved, while argon gas is continuously introduced to prevent oxidation of the melt [15]. The mechanism for achieving precise control of the melt solidification process via injection, forming, and pressure holding is illustrated in Figure 2. To validate the experimental conditions, the actual equipment setup (Model J5580) and the prepared tensile specimens are shown in Figure 3.

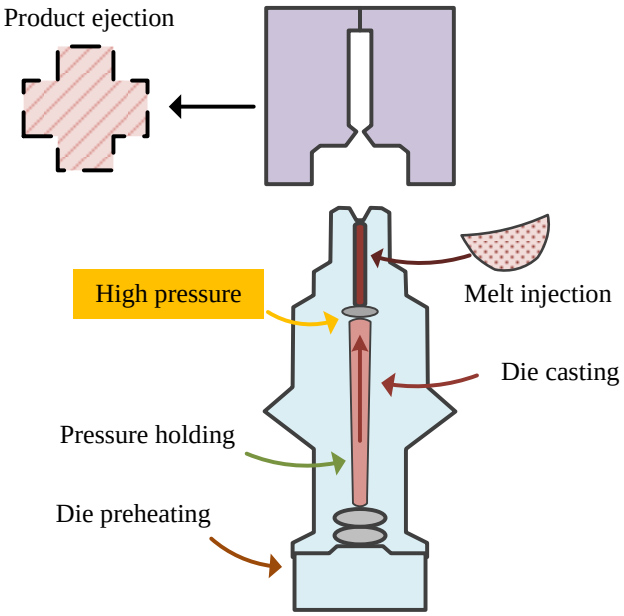

Figure 2. Schematic diagram of horizontal squeeze casting machine operation

(a) Extrusion casting machine (b) Tensile test specimen

Figure 3. Actual experimental setup

As shown in Figure 2 and 3, the core squeeze casting process was performed on a horizontal squeeze casting machine (Model J5580). First, the melt was injected into the preheated mold (220 ± 10 °C) to ensure filling performance. Subsequently, the injection plunger applied high pressure to eliminate filling defects and promote nucleation [16]. Crucially, the pressure was maintained for a specific holding time to suppress micropores and provide conditions for solute diffusion [17]. The key process parameters were rigorously controlled: pouring temperature was monitored by K-type thermocouples (± 2 °C), forming pressure was regulated by a closed-loop electro-hydraulic servo system (± 0.5 MPa), and holding time was controlled by the PLC system. The specific grouping of orthogonal experimental parameters for squeeze casting is shown in Table 2.

https://doi.org/10.64486/m.65.3.10

Table 2. Grouping table of orthogonal experiment parameters for squeeze casting

Experiment No. / **L9(34)Orthogonal Array**	**Pouring Temperature**	**Forming Pressure**	**Holding Time**
1	720 °C	90 MPa	5 s
2	720 °C	130 MPa	9 s
3	720 °C	170 MPa	13 s
4	730 °C	90 MPa	9 s
5	730 °C	130 MPa	13 s
6	730 °C	170 MPa	5 s
7	740 °C	90 MPa	13 s
8	740 °C	130 MPa	5 s
9	740 °C	170 MPa	9 s
Replicate Experiments	Pouring Temperature	Forming Pressure	Holding Time
10	720 °C	90 MPa	5 s
11	730 °C	130 MPa	13 s
12	740 °C	170 MPa	9 s

As shown in Table 2, to explore the synergistic regulation law of the three core process parameters of pouring temperature, forming pressure, and holding time on the uniformity of Al-Cu alloy solidification structure, a three factor three-level orthogonal experimental design method was adopted for the study. Samples were taken from the finished casting (diameter 50 mm × 100 mm) and processed into micro-characterization specimens (5 mm × 5 mm × 5 mm), microhardness specimens (10 mm × 10 mm × 10 mm), and tensile specimens conforming to GB/T 228.1-2021 (gauge length 25 mm, diameter 5 mm). All specimens were solution treated and then aged at 120 °C for 4 hours to promote uniform precipitation of the Al_2Cu phase. The precise characterization sampling scheme for the uniformity of casting structure and mechanical properties is shown in Figure 4.

https://doi.org/10.64486/m.65.3.10

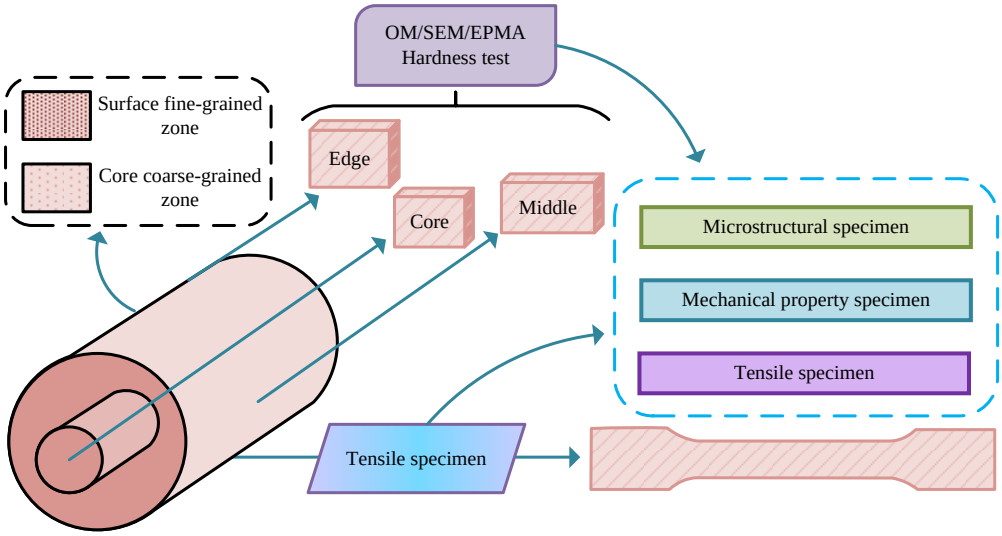

Figure 4. Schematic diagram of sample sampling location

As shown in Figure 4, the sampling scheme focuses on the radial direction of the casting. Microstructure samples were taken from the fine-grained surface zone and the coarse-grained core zone for analysis by optical microscopy (OM), scanning electron microscopy (SEM), and electron probe X-ray microanalysis (EPMA) to quantify the grain size standard deviation (GSSD) and the segregation degree of the Al_2Cu phase. Subsequently, samples from different radial positions were used for microhardness testing to evaluate hardness fluctuations and assess microstructural uniformity. Finally, a dog-bone-shaped tensile specimen was extracted from the center of the casting to evaluate the overall tensile strength.

2.3. Testing Methods for Uniformity of Solidification Structure and Mechanical Properties

A characterization scheme for microstructure and properties was developed to quantitatively evaluate the solidification structure. The analysis of solidification microstructure morphology was carried out using OM (model Olympus GX51) and SEM (model ZEISS Sigma 300). The OM sample was ground, polished with 1 μm diamond polishing paste, and etched with 0.5 % HF solution for 10 s. Grain size was measured using the intercept method (GB/T 6394-2017) across five non-overlapping fields of view to calculate the Grain Size Standard Deviation (GSSD). SEM testing was conducted with an acceleration voltage of 15 kV to observe the morphology and distribution of Al_2Cu phase precipitation. EPMA (Shimadzu EPMA-1720) was used for element concentration and phase segregation analysis. A line scan was performed along the radial direction (step size 1 μm, range 50 μm × 50 μm) to obtain the Cu concentration profile. The segregation degree of the Al_2Cu phase was calculated based on the Cu concentration data; a value less than 0.2 was considered uniform. The specific selection of EPMA line scanning and observation areas is shown in Figure 5.

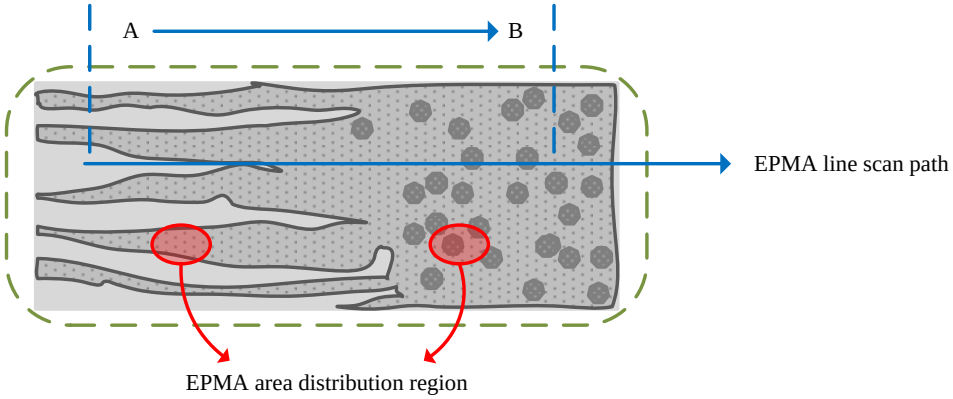

Figure 5. Schematic diagram of EPMA line scanning and observation area selection

https://doi.org/10.64486/m.65.3.10

As shown in Figure 5, the schematic diagram illustrates the strategy for EPMA line scanning and observation area selection, which focuses on typical microstructure features like grain boundaries to capture changes in local composition. Firstly, scan along the preset path to obtain the continuous variation curve of Cu concentration (peak corresponding to rich copper phase (Al_2Cu), valley corresponding to poor copper phase (α-Al)), providing a basis for quantifying segregation degree. Subsequently, a two-dimensional distribution map of Cu element is scanned in a specific area to verify the segregation of grain boundaries. The combination of line scan and surface scan ensures the comprehensiveness and accuracy of solidification segregation assessment, and its quantitative data can be compared with the actual composition of the alloy to evaluate the compositional deviation in the preparation process.

Mechanical performance testing included microhardness and tensile testing. Microhardness was tested using a Vickers hardness tester (model HVS-1000) with a load of 100 g (0.98 N) and a dwell time of 15 s. Each sample was measured at 5 points to calculate the standard deviation (SD) of hardness. Tensile testing was conducted on an electronic universal testing machine (model MTS C45.305) with a loading rate of 2 mm/min. Three parallel specimens were tested for each group, and the results are expressed as "mean ± SD".

3. Results

Based on the primary three-level orthogonal design, supplementary experiments were conducted at intermediate intervals—specifically at temperatures of 725 °C and 735 °C and refined time steps—to capture the non-linear evolution of the microstructure. These augmented datasets have been integrated into Figures 6, 7, and 8 to provide a continuous and precise trend analysis.

3.1. Influence of Process Parameters on Solidification Structure and Properties

In the squeeze casting process of Al-Cu alloy, the pouring temperature directly affects the temperature field of the melt, which in turn affects solute diffusion and grain growth processes. To clarify the independent control effect of this parameter on the solidification microstructure uniformity (GSSD, Al_2Cu phase segregation degree) and mechanical properties of Al-6.07wt.%Cu alloy, different process controls were studied as a single variable, and key parameters such as forming pressure and holding time were fixed according to experimental needs for exploration. The effect of pouring temperature on solidification structure and mechanical properties is shown in Figure 6.

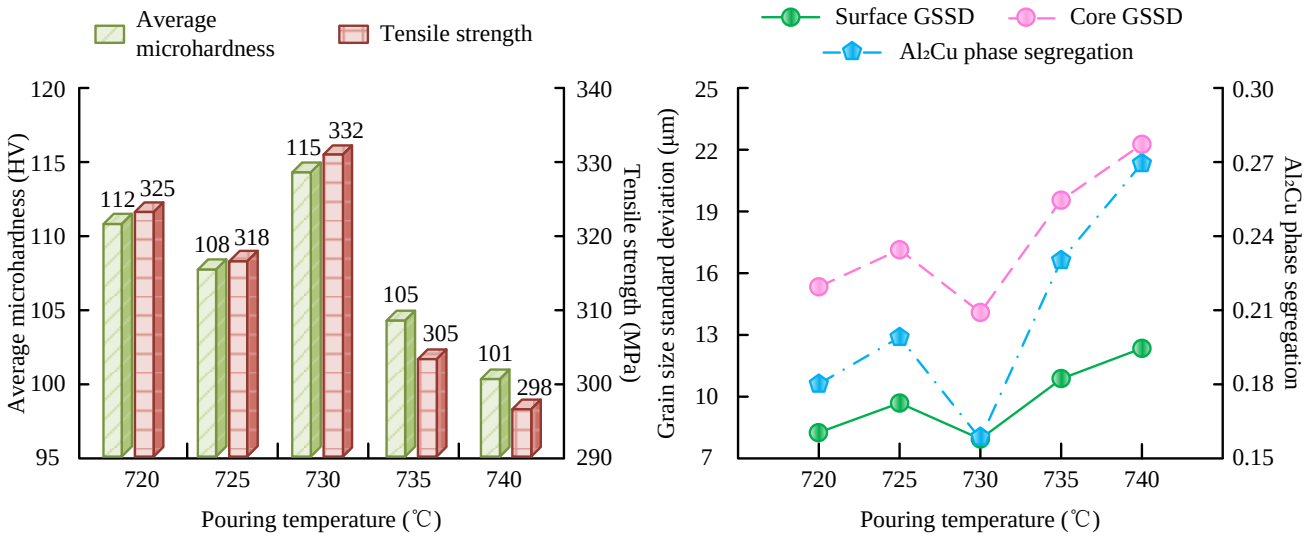

(a) Effect on average microhardness and tensile strength of Al-6.07wt.% Cu alloy

(b) Effect on grain size standard deviation and Al_2Cu phase segregation of Al-6.07wt.% Cu alloy

Figure 6. Effect of pouring temperature on solidification structure and mechanical properties

https://doi.org/10.64486/m.65.3.10

As shown in Figure 6 (a), when the pouring temperature was between 720 °Cand 740 °C the mechanical properties of Al-6.07 wt.% Cu alloy were optimal at 730 °C with an average microhardness of 115HV and a tensile strength of 332MPa. After the temperature deviated from 730 °C(above or below), the average microhardness and tensile strength both showed a decreasing trend, dropping to 101HV and 298MPa respectively at 740 °C indicating that the appropriate pouring temperature is the key to ensuring the stability of the alloy's mechanical properties.

As shown in Figure 6 (b), the uniformity of the alloy solidification structure was optimal at 730 °Cwith the lowest GSSD (surface 7.9 μm, core 14.2 μm) and Al_2Cu phase segregation degree (0.16). After temperature deviation, all three increased. At 740 °Cthe surface and core GSSD reached 12.3 μm and 22.1 μm, respectively, and the Al_2Cu phase segregation degree increased to 0.27, fully indicating that 730 °Ccan effectively alleviate the problem of tissue segregation. The effect of forming pressure on solidification structure and mechanical properties is shown in Figure 7.

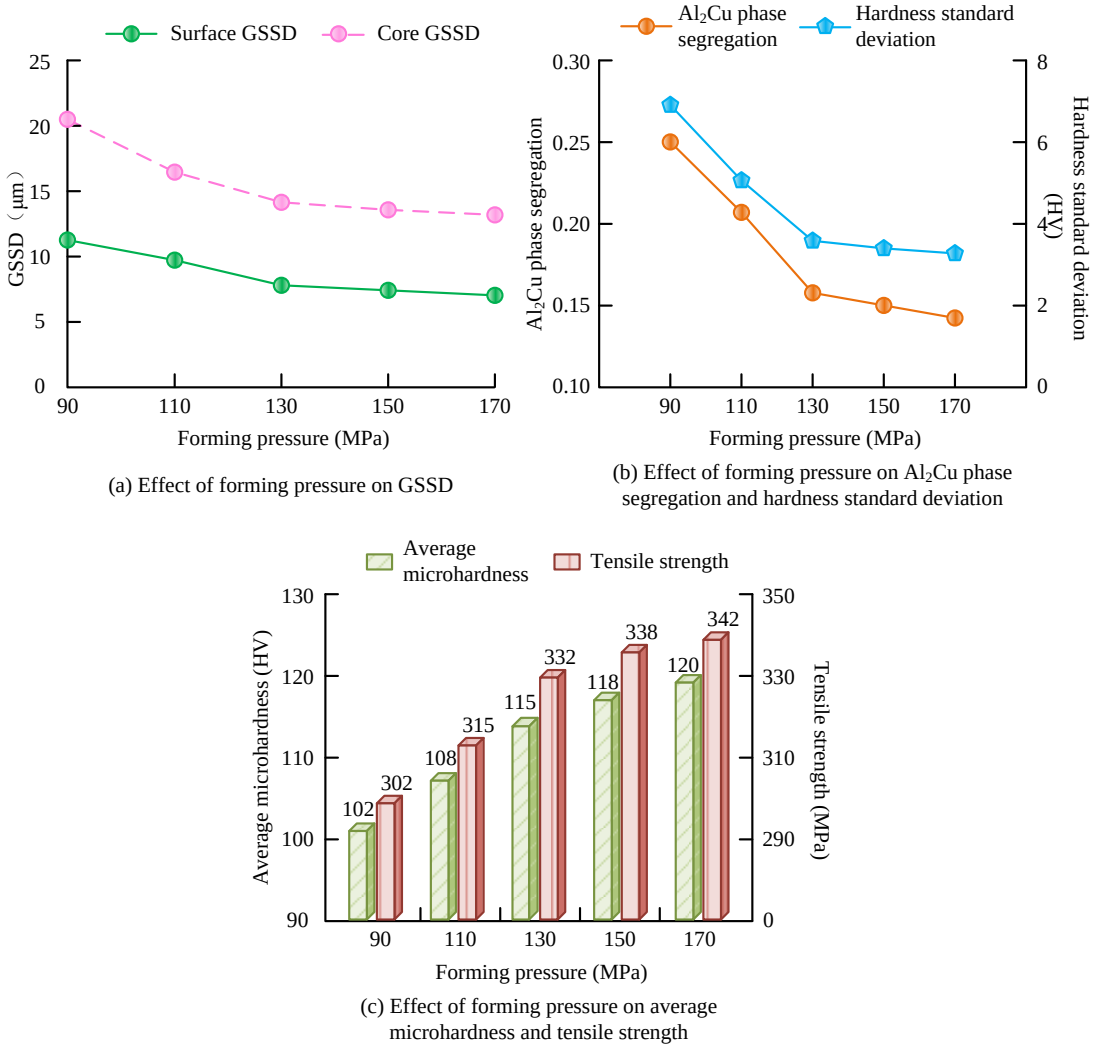

Figure 7. Effect of forming pressure on solidification structure and mechanical properties

As shown in Figure 7 (a), with the increase of forming pressure from 90MPa to 170MPa, the surface GSSD of Al-6.07 wt.%Cu alloy decreased from 11.5 μm to 7.3 μm, and the core GSSD decreased from 20.3 μm to 13.5 μm, significantly improving the uniformity of grain distribution. As shown in Figure 7 (b), the Al_2Cu phase segregation degree decreased from 0.25 to 0.14 (reaching a uniform standard of less than 0.2), and the hardness SD decreased from 6.8HV to 3.2HV, indicating that increasing pressure can reduce solute segregation and

https://doi.org/10.64486/m.65.3.10

decrease hardness fluctuations. As shown in Figure 7 (c), the average microhardness increased from 102HV to 120HV, and the tensile strength increased from 302MPa to 342MPa, indicating that optimizing the forming pressure can simultaneously improve the mechanical properties of the alloy. The effect of holding time on solidification structure and mechanical properties is shown in Table 3.

Table 3. Effect of holding time on solidification structure and mechanical properties

Holding time/s	Surface Layer Grain Size SD/μm	Core Grain Size SD μm	Al_2Cu Phase Segregation Degree	Average Vickers Hardness/HV	Hardness SD/HV	Tensile Strength MPa	Elongation %
5	10.3	18.7	0.26	105	6.5	310	7.2
7	8.9	16.4	0.22	110	4.8	320	7.9
9	7.9	14.2	0.16	115	3.8	332	8.5
11	7.6	13.9	0.15	117	3.4	335	8.4
13	7.5	13.7	0.14	118	3.2	337	8.3

In Table 3, when the holding time increased from 5s to 13s, the surface GSSD decreased from 10.3 μm to 7.5 μm, the core GSSD decreased from 18.7 μm to 13.7 μm, and the Al_2Cu phase segregation degree gradually decreased from 0.26 to 0.14. The average microhardness increased from 105 HV to 118 HV, the SD of hardness decreased from 6.5 HV to 3.2 HV, the tensile strength increased from 310 MPa to 337 MPa, and the elongation reached a peak of 8.5 % at 9 s and then slightly decreased to 8.3 %. This result confirms that extending the holding time can promote the diffusion of Cu element, and the regularity of the improvement in uniformity and performance slows down after 9 seconds is obtained.

Consistent with the effects of individual parameters (pouring temperature, forming pressure, holding time) discussed above, OM/SEM observations further revealed the microstructure and pore evolution: under non-optimal parameter combinations (e.g., pouring temperature 740 ℃forming pressure 90MPa, holding time 5s), OM images showed obvious core pores (2–5) μm in diameter and severe grain size imbalance (surface grain size ~25 μm, core grain size ~40 μm); SEM observations also found (5–10) μm needle-like Al_2Cu phases clustered at grain boundaries. In contrast, under the optimal parameters (730 ℃ pouring temperature, 170MPa forming pressure, 13s holding time, summarized from single-parameter results), porosity was significantly reduced to <0.5 % (pore diameter <1 μm), grains were refined and uniform (surface ~18 μm, core ~25 μm), and Al_2Cu phases transformed into (1–2) μm granular precipitates evenly dispersed in the Al matrix.

These microstructural changes directly explain why the optimal parameters achieved the lowest GSSD and Al_2Cu segregation degree, as well as the highest mechanical properties. After clarifying the independent control effect of single variables such as pouring temperature on the uniformity of solidification structure of Al-6.07wt.%Cu alloy, considering the interaction effect of process parameters in actual squeeze casting, and to further reveal the coupling mechanism of "pressure field-temperature field" proposed in the study, bivariate experiments were further conducted. The synergistic effect of pouring temperature and forming pressure on the solidification structure is shown in Table 4.

https://doi.org/10.64486/m.65.3.10

Table 4. The synergistic effect of pouring temperature and forming pressure on solidification structure.

Pouring Temperature/°C	Forming Pressure/MPa	Surface Layer Grain Size SD/μm	Core Grain Size SD/μm	Al_2Cu Phase Segregation Degree	Average Vickers Hardness/HV	Tensile Strength MPa
	90	9.8	17.5	0.23	108	315
720	130	8.5	15.1	0.19	113	328
	170	8.1	14.5	0.17	116	335
	90	11.5	20.3	0.25	102	302
730	130	7.9	14.2	0.16	115	332
	170	7.3	13.5	0.14	120	342
	90	13.2	23.5	0.30	98	295
740	130	10.8	19.5	0.23	105	305
	170	9.6	17.8	0.20	109	318

As shown in Table 4, the combination of 730 °C and 170 MPa yielded the optimal results, exhibiting the lowest surface and core GSSD values (7.3 μm and 13.5 μm, respectively), the minimum Al_2Cu phase segregation degree (0.14), and the highest average microhardness (120 HV) and tensile strength (342 MPa). When the pouring temperature deviated from 730 °C (i.e., 720 °C or 740 °C), increases in forming pressure were insufficient to compensate for the resulting deterioration in grain uniformity and mechanical properties. Similarly, at 730 °C with an insufficient forming pressure of 90 MPa, pronounced microstructural segregation was observed, with a segregation degree of 0.25. These results confirm the critical role of the synergistic interaction between the temperature field and pressure field in optimizing the solidification microstructure. The effects of aging temperature and aging time on the uniformity of Al_2Cu precipitation are presented in Table 5.

Table 5. Effects of aging temperature and aging time on the uniformity of Al_2Cu precipitation.

Aging Temperature/°C	Aging Time/h	Al_2Cu Phase Segregation Degree	Average Vickers Hardness/HV	Hardness SD/HV	Tensile Strength/MPa	Elongation/%
	2	0.21	108	4.2	318	8.0
110	4	0.18	112	3.6	325	8.3
	6	0.17	113	3.5	327	8.2
	2	0.19	110	3.9	322	8.1
120	4	0.16	115	3.8	332	8.5
	6	0.15	116	3.4	334	8.4
	2	0.22	106	4.5	315	7.8
130	4	0.20	109	4.1	320	7.6
	6	0.19	111	3.8	323	7.5

As shown in Table 5, the aging condition of 120 °C for 4 h exhibited the best overall performance, with the Al_2Cu phase segregation degree reduced to 0.16. Under these conditions, the average microhardness reached 115 HV, the tensile strength was 332 MPa, and the elongation attained 8.5 %, all representing peak values among the tested conditions. In addition, the hardness standard deviation was only 3.8 HV, indicating

https://doi.org/10.64486/m.65.3.10

enhanced microstructural uniformity. At an aging temperature of 110 °C, increasing the aging time from 2 h to 6 h led to a gradual decrease in the segregation degree from 0.21 to 0.17, accompanied by steady improvements in mechanical properties. In contrast, the specimens aged at 130 °C generally exhibited higher segregation degrees (> 0.19) and lower average hardness and tensile strength compared with those aged at 120 °C. These results indicate that appropriate aging parameters promote the uniform precipitation of the Al_2Cu phase and confirm the critical role of bivariate synergistic regulation in enhancing microstructural uniformity and mechanical performance.

After establishing the regulatory effect of holding time on the solidification microstructure uniformity of the Al–6.07 wt.% Cu alloy, and considering its central role as a key process variable, the holding time interval was further refined to more accurately capture its dynamic influence on GSSD and Al_2Cu phase segregation. This approach enabled a deeper verification of the solute-field-driven Cu diffusion mechanism within the proposed "pressure field–temperature field–solute field" coupling framework. The corresponding results are presented in Figure 8.

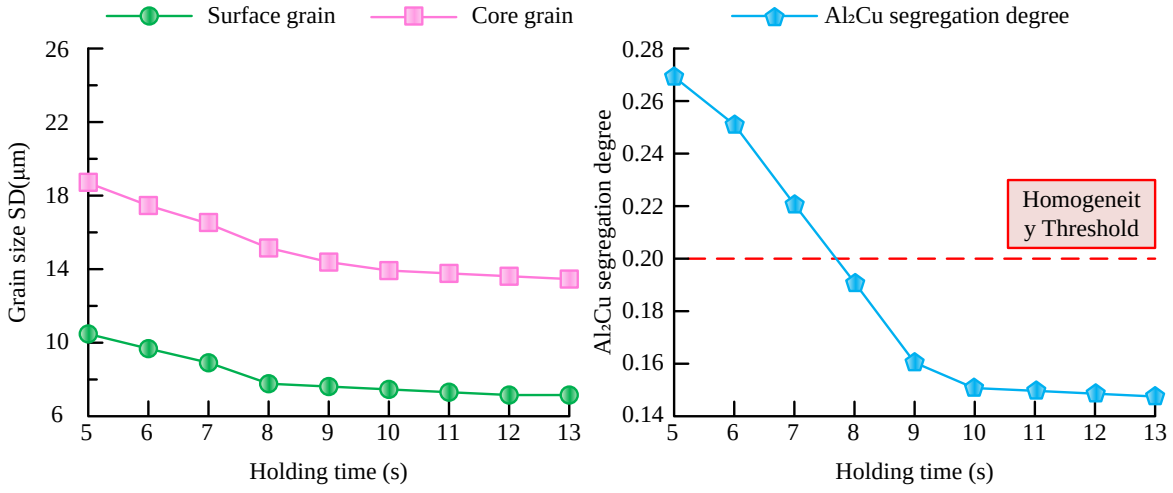

(a) Effect of holding time on grain size SD

(b) Effect of holding time on segregation degree of Al_2Cu phase

Figure 8. Effect of holding time on core uniformity index.

As shown in Figure 8 (a), as the holding time increased from 5 s to 13 s, the surface GSSD of Al-Cu alloy decreased from 10.3 μm to 7.5 μm, and the core GSSD decreased from 18.7 μm to 13.7 μm. In the (5-9) s stage, both showed a significant decrease (surface decrease of 2.4 μm, core decrease of 4.5 μm), and the decrease slowed down after 9 s, indicating that the pressure retention had a prominent effect on improving grain uniformity during this stage. After 9 s, solute diffusion became more complete, and the optimization effect of uniformity weakened. As shown in Figure 8 (b), the segregation degree of Al_2Cu phase decreased from 0.27 at 5 s to 0.14 at 13 s, and from 0.27 to 0.16 at (5-9) s, with a significant decrease. After 11 s, it stabilized at 0.14 (less than 0.2, judged as uniform), confirming that the extension of holding time promoted Cu diffusion and optimized the uniformity of Al_2Cu precipitation.

3.2. Microstructural Analysis

Consistent with the mechanical property trends, the evolution of the microstructure provides direct evidence for the property enhancement. The representative optical microstructures of the sample prepared under the optimal parameters (730 °C, 170 MPa, 13 s) are presented in Figure 9.

https://doi.org/10.64486/m.65.3.10

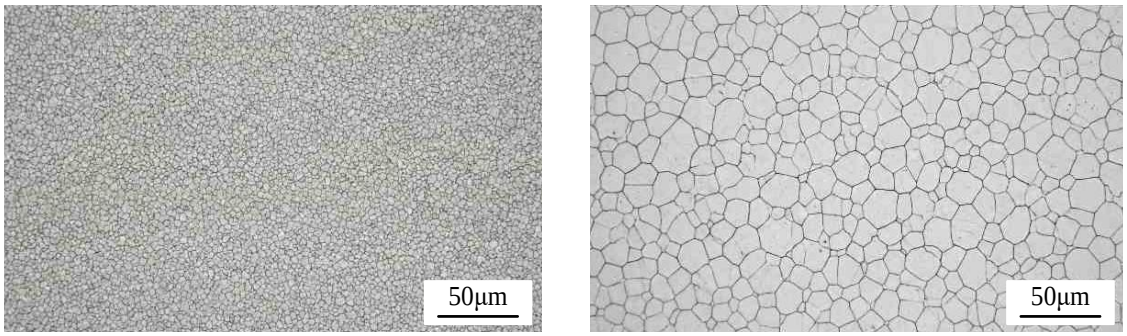

(a) Surface area (b) Core Area

Figure 9. Representative optical microstructures.

As observed in Figure 9, the distinct difference between the surface and core regions is clearly revealed. The surface layer (Figure 9a) consists of fine, dense grains formed due to the rapid cooling rate and high applied pressure. In contrast, the core area (Figure 9b) exhibits slightly coarser but uniform equiaxed grains. Importantly, this structure effectively avoids the "coarse dendrite" defects and shrinkage porosity often seen in traditional casting, confirming the efficacy of the parameter optimization. To further investigate the strengthening mechanism, SEM characterization was conducted to observe the morphology of the second phase. The SEM micrographs of the Al_2Cu precipitates after aging at 120 °C for 4 h are shown in Figure 10.

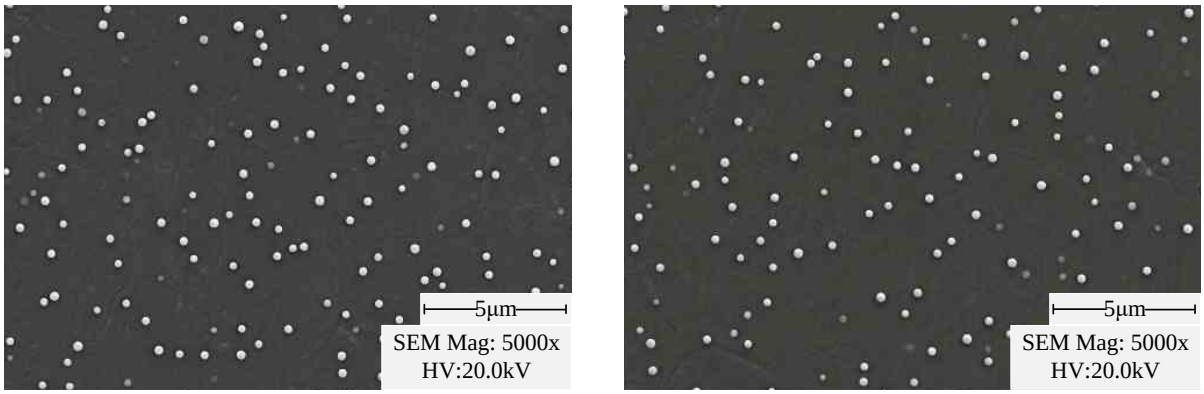

(a) (b)

Figure 10. SEM micrographs showing Al_2Cu.

As shown in Figure 10, unlike the coarse net-like structures typically found in unoptimized samples, the Al_2Cu phase in the optimized alloy appears as fine, granular precipitates evenly dispersed within the α-Al matrix, as detailed in Figure 10b. This dispersion strengthening effect, facilitated by the fragmentation of the dendritic network under high pressure, is a key factor contributing to the achieved high tensile strength of 342 MPa. Finally, to quantify the chemical homogeneity and verify the suppression of segregation, EPMA line scanning was performed across the grain boundaries. The resulting Cu concentration profile is illustrated in Figure 11.

https://doi.org/10.64486/m.65.3.10

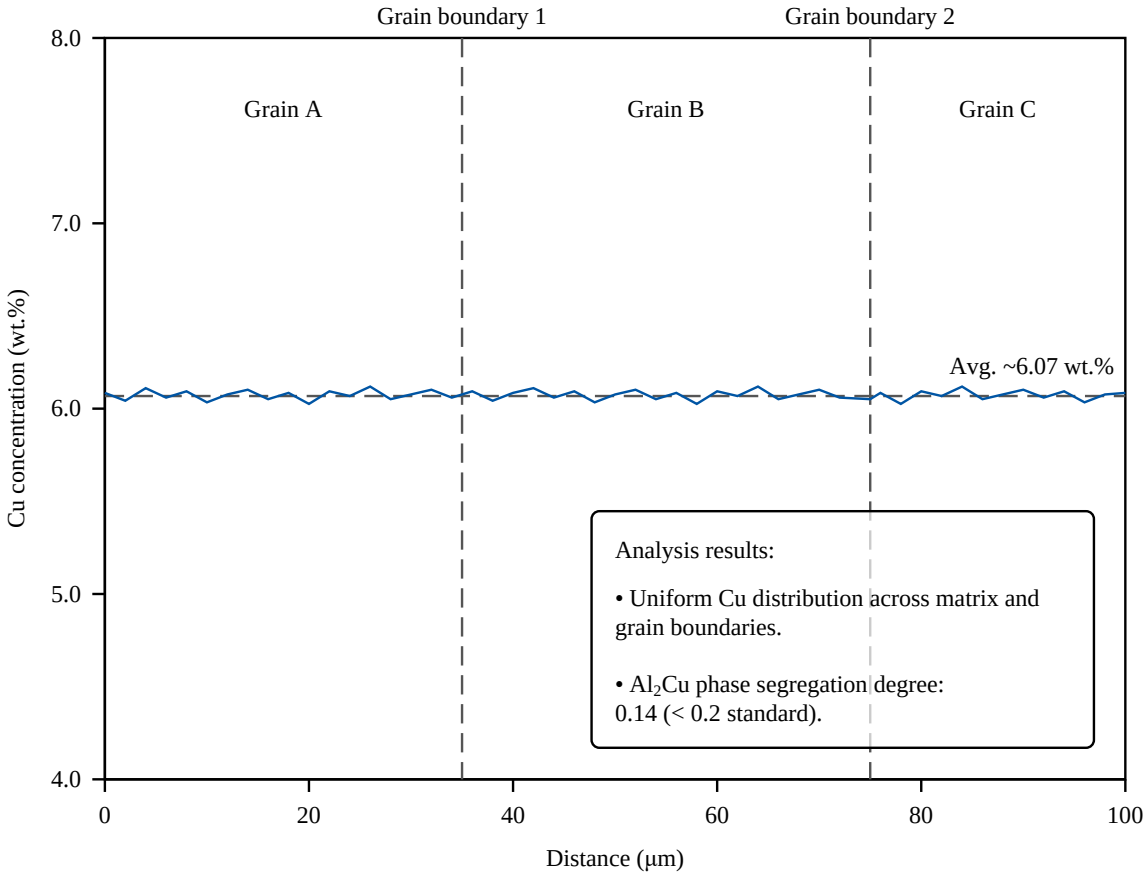

Figure 11. EPMA line scan profile.

As shown in Figure 11, the Cu concentration fluctuates stably around the average composition of 6.07 wt.%, without significant enrichment peaks at the grain boundaries. The calculated Al_2Cu phase segregation degree is only 0.14, which fully satisfies the uniformity standard (< 0.2). This quantitative evidence confirms that the synergistic control of pressure and holding time effectively promoted solute diffusion and suppressed macro-segregation.

4. Discussion

The study successfully improved the solidification microstructure uniformity of Al-6.07wt.%Cu alloy via squeeze casting optimization. Under the optimal parameters (730 °C, 170 MPa, 13 s), the "pressure-temperature-solute" coupling mechanism played a decisive role. The forming pressure of 170 MPa effectively fragmented coarse dendrites, while the pouring temperature of 730 °C provided an ideal thermodynamic environment for nucleation. Crucially, the extended holding time (13 s) facilitated the full diffusion of Cu elements, suppressing the grain boundary enrichment of the Al_2Cu phase.

This mechanism is supported by the microstructural evolution observed in Figures 9–11, where the transformation from coarse dendrites to fine equiaxed grains and dispersed granular Al_2Cu precipitates was evident. Consistent with the findings of Hu et al. [18], the stress field significantly influenced the directional distribution of precipitates, promoting uniformity. Additionally, the quantitative evaluation standards (GSSD and segregation degree) established in this work provide experimental validation for the phase-field simulation models proposed by Zhao et al. [19], bridging the gap between theoretical microstructure design and engineering application. Furthermore, unlike Zhang et al. [20], who focused primarily on defect elimination via secondary loading, this study quantified uniformity using GSSD and segregation degree, proving that multi-parameter synergy offers superior control over micro-segregation compared to single-factor regulation.

https://doi.org/10.64486/m.65.3.10

5. Conclusion

(1) A three-factor orthogonal experimental design identified the optimal squeeze casting parameters for the Al–6.07 wt.% Cu alloy: a pouring temperature of 730 °C, a forming pressure of 170 MPa, and a holding time of 13 s, followed by aging at 120 °C for 4 h. (2) Under these conditions, the grain size standard deviation (GSSD) of the surface and core reached 7.3 μm and 13.5 μm, respectively, while the Al_2Cu phase segregation degree was minimized to 0.14. (3) The suppression of macrosegregation and the uniform dispersion of granular Al_2Cu phases increased the tensile strength to 342 MPa and the microhardness to 120 HV. (4) This study validates the proposed "pressure–temperature–solute" coupling mechanism and provides a robust process route for manufacturing high-quality, high-load-bearing aerospace components.

Future work will extend the parameter range to investigate the effects of ultra-high forming pressures (> 200 MPa).

References

[1] S. Fan, X. Guo, Z. Li, J. Ma, F. Li, and Q. Jiang, "A review of high-strength aluminum-copper alloys fabricated by wire arc additive manufacturing: microstructure, properties, defects, and post-processing," *Journal of Materials Engineering and Performance*, vol. 32, no. 19, pp. 8517-8540, 2023, https://doi.org/10.1007/s11665-023-08233-5

[2] D. Kim and H. Youn, "Classifying roundness and sphericity of sand particles using CNN regression models to alleviate data imbalance," *Acta Geotechnica*, vol. 19, no. 10, pp. 6569-6584, 2024, https://doi.org/10.1007/s11440-024-02410-z

[3] L. B. Ma, W. J. Cheng, X. L. Guo, B. Z. Fan, Y. Guan, Y. P. Li, L. Jin, G. Y. Shui, Y. Z. Jiang, and X. Sun, "A new vacuum-assisted low-pressure investment casting process for K446 alloy," *China Foundry*, vol. 21, no. 6, pp. 702-708, 2024, https://doi.org/10.1007/s41230-024-3148-0

[4] Y. Yuan, Y. Yang, Z. Wang, Q. He, K. Sun, and R. Fan, "Epsilon-negative materials with lower percolation threshold derived from segregated structures," *Polymer Composites*, vol. 45, no. 18, pp. 16706-16715, 2024, https://doi.org/10.1002/pc.28922

[5] W. Yuan, H. D. Zhao, X. Shen, C. Zou, Y. Liu, and Q. Y. Xu, "Numerical simulation of microstructure and microporosity morphology in directional solidification of aluminum-copper alloys: Effect of copper content and withdrawal rate," *China Foundry*, vol. 22, no. 1, pp. 33-44, 2025, https://doi.org/10.1007/s41230-024-4014-9

[6] W. Suprapto, Y. S. Irawan, S. Suparman, M. R. Amrullah, P. Auliasyah, and A. R. Ramdhani, "The effect of hold-melt time of micro-regime precipitation size and hardness in Al-Cu alloy," *EUREKA: Physics and Engineering*, vol. 2, pp. 222-234, 2023, https://doi.org/10.21303/2461-4262.2023.002684

[7] X. Peng, X. X. Li, R. C. Wang, Y. Feng, S. J. Yan, and Z. Y. Cai, "Anisotropy of rapidly solidified 2195 alloy rolled sheets: Effect of pre-thermal treatment prior to rolling and aging treatment," *Journal of Central South University*, vol. 32, no. 5, pp. 1660-1677, 2025, https://doi.org/10.1007/s11771-025-5979-2

[8] Y. Tan, H. Zhao, and Q. Xu, "Numerical simulation of solidified microstructure of ternary Al-Si-Mg alloy using an improved cellular automaton method," *Science China Materials*, vol. 67, no. 4, pp. 1150-1159, 2024, https://doi.org/10.1007/s40843-023-2706-x

[9] R. Bhadrinath, R. Saravanan, R. Vaira Vignesh, A. Shanmugasundaram, and M. Govindaraju, "Tribological and corrosion characteristics of aluminium–copper alloys reinforced with alumina nickel aluminide cermet powder," *Corrosion Engineering, Science and Technology*, vol. 60, no. 4, pp. 276-289, 2025, https://doi.org/10.1177/1478422X241288800

[10] J. V. de Sousa Araujo, I. Costa, and X. Zhou, "Comparison of constituent intermetallic particles in different aluminium alloys," *Metallography, Microstructure, and Analysis*, vol. 14, no. 1, pp. 106-119, 2025, https://doi.org/10.1007/s13632-025-01170-w

[11] Y. Elmoghazy, E. M. O. Abuelgasim, S. A. Osman, Y. R. H. Afaneh, O. M. A. Eissa, and B. Safaei, "Effective mechanical properties evaluation of unidirectional and bidirectional composites using virtual domain approach at microscale," *Archives of Advanced Engineering Science*, vol. 1, no. 1, pp. 27-37, 2023, https://doi.org/10.47852/bonviewAAES32021723

https://doi.org/10.64486/m.65.3.10

[12] L. L. Lu, H. T. Liu, Z. D. Wang, Q. Q. Lu, Y. J. Zhou, F. Zhou, Y. M. Zhang, W. W. Lu, B. Yang, Q. Q. Zhu, and K. X. Song, "Advances in electrolytic copper foils: Fabrication, microstructure, and mechanical properties," *Rare Metals*, vol. 44, no. 2, pp. 757-792, 2025, https://doi.org/10.1007/s12598-024-02965-6

[13] K. Suchan, J. Just, P. Beblo, C. Rehermann, A. Merdasa, R. Mainz, I. G. Scheblykin, and E. Unger, "Multi-stage phase-segregation of mixed halide perovskites under illumination: A quantitative comparison of experimental observations and thermodynamic models," *Advanced Functional Materials*, vol. 33, no. 3, pp. 2206047, 2023, https://doi.org/10.1002/adfm.202206047

[14] F. Yilan, R. Ekici, and L. Urtekin, "Recent advances in the AlSi10Mg materials fabrication by selective laser melting: Process parameters, optimization, low-velocity and ballistic impact responses," *Progress in Additive Manufacturing*, vol. 10, no. 8, pp. 4305-4325, 2025, https://doi.org/10.1007/s40964-024-00856-x

[15] M. Bharathwaj, S. Sugunraj, P. Karuppasamy, M. Srinivasan, and P. Ramasamy, "Effect of argon flow rate on mc-silicon ingot grown by DS process for PV application: A numerical investigation of non-metallic impurities," *Silicon*, vol. 15, no. 14, pp. 5937-5946, 2023, https://doi.org/10.1007/s12633-023-02490-8

[16] P. Li, S. Xia, J. Dong, L. Dai, Z. Luo, and K. Xue, "Effect of bimodal quasicrystal phase on the dynamic recrystallization of Mg–Zn–Gd alloy during high-pressure torsion," *Acta Metallurgica Sinica (English Letters)*, vol. 37, no. 7, pp. 1128-1134, 2024, https://doi.org/10.1007/s40195-024-01687-z

[17] S. Asnaashari, M. Shateri, A. Hemmati-Sarapardeh, and S. S. Band, "Modeling of the sintered density in Cu-Al alloy using machine learning approaches," *ACS Omega*, vol. 8, no. 31, pp. 28036-28051, 2023, https://doi.org/10.1021/acsomega.2c07278

[18] W. Hu, J. Chen, S. Han, J. Xu, J. Miao, T. Xing, and R. Guan, "Initial report on the oriented-precipitation of T1-phase in creep-aged Al-Cu-Li single crystal," *Metals and Materials International*, vol. 29, no. 5, pp. 1382-1389, 2023, https://doi.org/10.1007/s12540-022-01307-4

[19] Y. Zhao, T. Xin, S. Tang, H. Wang, X. Fang, and H. Hou, "Applications of unified phase-field methods to designing microstructures and mechanical properties of alloys," *MRS Bulletin*, vol. 49, no. 6, pp. 613-625, 2024, https://doi.org/10.1557/s43577-024-00720-x

[20] Z. Zhang, M. Gao, Y. Ning, and R. Guan, "Improving the defects and mechanical properties via secondary loading in a squeeze casting heat-treated Al–Cu alloy," *Journal of Materials Research and Technology*, vol. 36, pp. 2971-2976, 2025, https://doi.org/10.1016/j.jmrt.2025.03.265

 https://doi.org/10.64486/m.65.3.10